

# Design and feasibility study of novel paraboloid graphite based microbial fuel cell for bioelectrogenesis and pharmaceutical wastewater treatment

Tazien Rashid<sup>1</sup>, Farooq Sher<sup>2\*</sup>, Abu Hazafa<sup>3</sup>, Rizwan Qureshi Hashmi<sup>4</sup>, Ayesha Zafar<sup>5</sup>, Tahir Rasheed<sup>6</sup>, Sadiq Hussain<sup>4</sup>

<sup>1</sup>*Department of Chemical Engineering, NFC Institute of Engineering and Fertilizer Research Faisalabad, Pakistan*

<sup>2</sup>*School of Mechanical, Aerospace and Automotive Engineering, Faculty of Engineering, Environmental and Computing, Coventry University, Coventry CV1 5FB, UK*

<sup>3</sup>*Department of Biochemistry, University of Agriculture, Faisalabad, 38000, Pakistan*

<sup>4</sup>*Department of Chemical Engineering NFC Institute of Engineering and Technology, Multan, Pakistan*

<sup>5</sup>*Institute of Biochemistry and Biotechnology, Faculty of Biosciences, University of Veterinary and Animal Sciences, Lahore, Pakistan*

<sup>6</sup>*School of Chemistry and Chemical Engineering, Shanghai Jiao Tong University, Shanghai, 200240, China*

\*Corresponding author:

E-mail address: [Farooq.Sher@coventry.ac.uk](mailto:Farooq.Sher@coventry.ac.uk) (F.Sher)

Tel.: +44 (0) 24 7765 7754

## Abstract

The pharmaceutical industrial wastewater (PIW) is rising globally as one of the major health problems nowadays, not only for aquatic animals but also for human beings and the environment. Several conventional techniques including coagulation, filtration, biological membranes, and advanced oxidations have been used for the treatment of PIW, but all these techniques are limited with their applications and results. The present study aimed to build a cost-effective, high biodegradable, eco-friendly, and highly efficient PIW treatment technique to generate electricity and reduce the COD of wastewater. In the present study, the novel paraboloid of graphite-based microbial fuel cell (MFC) configuration has been designed, by

33 eliminating different types of casings and the membranes, for the bio-electrogenesis and the  
34 treatment of the PIW. Municipal solid wastewater (MSW) was used as the substrate for  
35 developing the biofilm in the paraboloid graphite-based MFC. The PIW treatment showed  
36 adequate bioelectricity generation including current, power, and voltage, and open-circuit  
37 voltage (OCV) of about 2.76 mA and 0.76 mW, 276 mV and 330 mV at 100  $\Omega$  respectively  
38 after five operating cycles. The cyclic voltammetry showed the maximum generation of 2.01  
39 W/m<sup>3</sup> and 168 mA/m<sup>2</sup> of power and current densities respectively followed by a considerable  
40 reduction in internal resistance from 197 to 99  $\Omega$ . The results reported a significant amount of  
41 reduction in COD and TDS of 80.55% (5460 to 1060 mg/L) and 35.62% (800 to 515 mg/L)  
42 respectively of PIW by MFC. The reduction in the % removal efficiency of the COD (80.55%)  
43 suggested that the removal of organic compounds from PIW is parallel to bioelectrogenesis.  
44 Based on these major findings, it is recommended the novel membrane-less and paraboloid  
45 graphite-based MFC operation significantly drag concentration towards the feasibility of using  
46 pharmaceutical wastewaters for bio-electrogenesis.

47 **Keywords:** Paraboloid-shaped MFC; Bioelectrogenesis; COD reduction; Pharmaceutical  
48 wastewater; Open circuit voltage and Power density.

## 49 **1 Introduction**

50 With the increasing world population, industrialization, and urbanization the demand for a  
51 quality life is also increasing. Several industries are established to fulfil the requirement of  
52 human beings, but along with their benefits, there are several types of problems including the  
53 production of wastewater [1]. The whole world is encountering several types of industrial  
54 effluents, which can exert many harmful effects including cancer, reproductive disorder, and  
55 organ failure. Among them, the most important are fertilizer, food and dairy processing,  
56 petrochemical, textile, and pharmaceutical effluents [2]. The pharmaceutical effluent is quite  
57 different from the rest of the conventional effluents due to discharging of organic pollutants

58 and drugs components including antibiotics, vitamins, antiepileptics and cosmetic ingredients  
59 and their adverse effects on the environment are not well known and are becoming one of the  
60 major problems for the environment and its stakeholders [3].

61

62 The pharmaceutical effluents contain a large amount of waste products including organic  
63 solvents, solid and liquid wastes, contaminants hormones, antiepileptic drugs, and antibiotics,  
64 which carried high total dissolved solids (TDS), chemical oxygen demand (COD), biochemical  
65 oxygen demand (BOD), and suspended solids. The waste containing a high amount of COD,  
66 when discharged into the streaming water, immediately reduces the dissolved oxygen and  
67 contaminates the water for further use [4]. Therefore, there is a need to decontaminate the  
68 pharmaceutical waste before discharging [5, 6]. The treatment of pharmaceutical waste is a  
69 very challenging task due to its intractable behaviours. Conventionally several techniques  
70 including chemical coagulation, osmosis, membrane techniques, advanced oxidation, and  
71 electronic coagulation have been used for the treatment of pharmaceutical wastewater, but all  
72 of these strategies did not attain considerable importance due to their limitations including less  
73 efficiency, low biodegradability, less reduction in COD and BOD of wastewater, and high cost  
74 [7].

75

76 Chemical coagulation is a simple wastewater technique [8], which involves destabilizing the  
77 contaminated water by using chemicals like ferric salts, lime, and aluminium sulphate, but few  
78 important concerns are about the formation of aggregation of compounds during the physical  
79 transportation of particles, low removal of pathogens, use of lethal chemicals, and  
80 environmental challenges [9, 10]. Another, conventional pharmaceutical wastewater treatment  
81 method is the reduction/oxidation in the bio-electrochemical system, which provides a suitable  
82 environment for the treatment of trace organic compounds in pharmaceutical wastewater, but

83 its major concerns are about the high cost and being less eco-friendly, and low bio-  
84 degradability difficulties [11]. Furthermore, the biological pharmaceutical wastewater  
85 treatment is also considered an important key strategy to treat the water, the microorganisms  
86 are used in most of the biological methods to degrade the contaminants into harmless water  
87 and carbon dioxide. But in the biological degradation systems. some parameters including  
88 limited removal of suspended solids, high hydraulic retention time, insufficient removal of  
89 turbidity, and biological degradation constant need to be addressed ( $K_{\text{biol}}$  is not present for  
90 many of the pharmaceutically active compounds including carbamazepine and clofibrac acid)  
91 to estimate the degradation efficiency of pharmaceutical wastewater [10, 12].

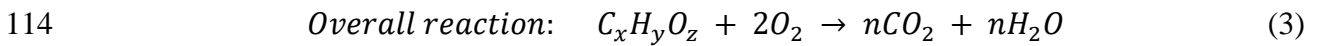
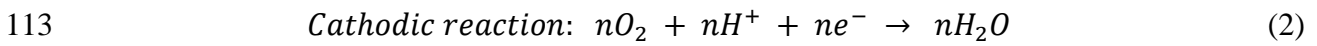
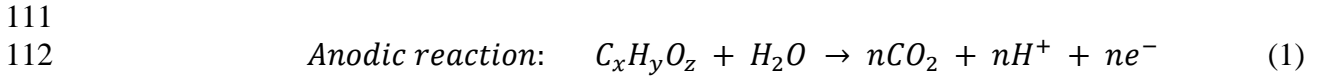
92

93 However, there is a need to develop a cost-effective, high degradable, and eco-friendly  
94 pharmaceutical wastewater treatment strategy. Recently, the microbial fuel cell (MFC) has  
95 attained considerable attention towards the treatment of wastewater including pharmaceutical  
96 wastewater due to its high degradation efficiency, multidirectional applications, the current  
97 generation, eco-friendly behaviour, and cost-effectiveness. Microbial fuel cell (MFC)  
98 technology is the bioreactor that depends on the electroactive bacteria, popularly known as  
99 exoelectrogens, to simultaneously produce electric power and treat wastewater by reducing the  
100 BOD and COD of effluents [13]. Design feasibility, energy production, power density, and  
101 scale-up of MFC are the major concerns of researchers to treat wastewater [14].

102

103 Initially, the double chamber microbial fuel cell was made which consisted of two  
104 compartments including anode and cathode. The anode chamber was filled with wastewater in  
105 which microbes break the organic compounds to produce the carbon dioxide along with  
106 hydrogen ions (proton) and electrons. Protons migrated to the cathodic chamber by proton  
107 exchange membrane (PEM) while electron transmitted to the cathode through an external

108 circuit where oxygen reduction occurs. The reactions between oxygen, hydrogen ion, and  
109 electron produce water (**Eqs.(1-3)**). The oxidation occurs in the anodic chamber while  
110 reduction occurs in the cathodic chamber [15, 16].



115  
116 The overall reaction involves the conversion of acetate into two components carbon-dioxide  
117 and water. According to emerging evidence, several types of MFC's including double chamber  
118 [15], cube and flat type [17], miniature, tubular [18], stacked [19], cylindrical [20], H-type [21],  
119 and single chamber [22] MFCs have been reported so far for the treatment of textile, dyes, and  
120 pharmaceutical wastewater. In cube and flat microbial fuel cells, the internal resistance is  
121 reduced by availing the large membrane area and inertly shorter distance between electrodes  
122 to increase the power production [17].

123  
124 Flat plate type MFC with Nafion PEM (proton exchange membrane) and anode assembly  
125 provides a larger surface area for membrane and cathode. The proton exchange membrane in  
126 cells significantly helped in transfer the chemical energy into electrical energy produced by the  
127 electrochemical reaction of oxygen and hydrogen, and also oppose the direct combustion of  
128 oxygen and hydrogen into thermal energy. The anodic chamber is usually fed with organic  
129 biomass while air is pumped through a cathodic chamber without using any liquid catholyte  
130 [23]. Single chamber microbial fuel cell has an external cathodic wall that is exposed to the  
131 atmosphere and eliminates the cost of oxygen (aeration) pumping to the cathodic chamber [22].  
132 A stacked microbial fuel cell consists of more than two chambers that can be applied in series  
133 or parallel form in order to increase the power up to 35 V [19]. The voltage reversal and limited  
134 power density are the major problems in the conventionally used MFC, in addition, these

135 microbial fuel cells have the lowest columbic efficiency and used membrane for ion exchange  
136 that provides greater resistance and cost as well [24].

137

138 Nayak and Ghosh [16] reported that photosynthetic microbial fuel cells showed the maximum  
139 COD removal of about 87.8% with an efficiency of 95% for pharmaceutical wastewater. They  
140 also revealed that pharmaceutical wastewater treatment produces maximum power density and  
141 voltage of 838.68 mW/m<sup>2</sup> and 740.13 mV respectively. Zhuang et al., [19] performed an  
142 experiment to treat real wastewater by parallel stack microbial fuel cell (PSMFC) at two  
143 different organic loading rates as 1.2 and 4.9 kg COD/m<sup>3</sup> d. They stated that PSMFC removed  
144 up to 90.8 and 83.8% of NH<sub>4</sub><sup>+</sup>-N and COD of wastewater at 1.2 kg COD/m<sup>3</sup> d and 80.7 and  
145 77.1% NH<sub>4</sub><sup>+</sup>-N and COD at 4.9 kg COD/m<sup>3</sup> d. They also observed maximum power density  
146 and voltage of 175.7 W/m<sup>2</sup> and 1.8 V respectively at 4.9 kg COD/m<sup>3</sup> d. Mohanakrishna et al.,  
147 [20] investigated the treatment of Labanah whey wastewater using cylindrical graphite  
148 microbial fuel cell and observed the maximum substrate deprivation efficiency of 72.76% with  
149 maximum power and current generation of 1.02 mW and 3.2 mA respectively at 100 Ω. Prasad  
150 and coworkers reported the maximum COD reduction of 91.50% with power generation of 335  
151 mV during pharmaceutical wastewater treatment by microbial fuel cell after a hydraulic  
152 retention period of 12 days [25]. Similarly, Amari and his research group observed the  
153 maximum COD reduction of 93 and 78%, and power density of 20.5 and 6.5 W/m<sup>3</sup> for real and  
154 synthetic wastewater respectively by dual-chambered microbial fuel cell [26].

155

156 In recent years, the pharmaceutical effluent is continuously increasing in its bulk and strength  
157 too. However, there is a need to develop a new and revolutionary technique to identify the  
158 complex mixture in pharmaceutical effluents and treat them effectively with high accuracy and  
159 less costly. To the best of our knowledge, for the first time, the present study evaluates the

160 formation of graphite-based, paraboloid shaped microbial fuel cell to generate greater  
161 electricity and reduce the total dissolved solids (TDS) and chemical oxygen demand (COD) of  
162 pharmaceutical wastewater. Moreover, for the first time, the substrate degradation rate (SDR)  
163 and organic loading rate (OLR) of pharmaceutical wastewater is discussed for a better  
164 understanding. The present study investigates the production of open-circuit voltage (OCV),  
165 current, power density, voltage, and current density from the pharmaceutical industrial  
166 wastewater by MFC.

## 167 **2. Materials and methods**

### 168 **2.1. Sample collection**

169 This pharmaceutical wastewater samples were taken from NabiQasim Pharma Industries,  
170 Karachi, Pakistan. Wastewater having the COD of 5460 mg/L and pH 7.4–7.7 was taken to the  
171 laboratory and quickly stored at 4 °C in the refrigerator. The aim of storing at 4 °C was to  
172 preserve the nature of the wastewater and to avoid any sort of biological change. Paraboloid  
173 shaped graphite based MFC was constructed for the treatment of pharmaceutical wastewater.  
174 Sodium acetate (99.9% purity) and phosphate buffer (pH 7) were purchased from the SIGMA-  
175 Aldrich Chemical Co. (USA).

### 176 **2.2. MCF configuration and inoculation**

177 The microbial fuel cell (MFC) was designed with a novel configuration that has a paraboloid  
178 shape. The paraboloid MFC was composed of two cups, one is the inner paraboloid cup named  
179 as a cathode and the other is the outer paraboloid cup named as the anode. Both anode and  
180 cathode were fabricated with the graphite material to remove any substrate effect. The anode  
181 and cathode were adjusted in one another in such a way that they showed truncated. The smaller  
182 paraboloid cup (cathode) was placed inside the larger paraboloid cup (anode), in such a way  
183 that the cathode placed epi-centrally in the anode. The anode electrode had the dimensions

184 of 108 mm height and 66 mm face diameter, while the cathode electrode had the dimensions  
185 of 85 mm height and 58 mm face diameter. The base of an anode (7 mm thick) and a cathode  
186 (3.5 mm) was made of graphite.

187

188 The open portion of space between the anode and the cathode (at the top) was closed with an  
189 acrylic plastic plate type ring, as shown in **Fig. 1**. The acrylic made plastic ring (lid) of the  
190 anode has two openings, one opening is used for the sampling purpose, and the second opening  
191 used for the feeding purpose. Both openings are of 1.5 mm in diameter, through which the tube  
192 of white plastic (1.5 mm diameter) inserted into the anode, and the opening of the tubes was  
193 kept closed throughout the operation for ensuring the anaerobic condition in the anode. The  
194 outer surface of the anode which is open to air was insulated with the paraffin layer to stop the  
195 environmental interference to the anolyte or the bioactivity inside the anode. This novel design  
196 of the MFC gives the dual truncated membrane-less MFC.

197

198 The apparent volume of the anode was 186 mL and the geometric surface area was measured  
199 as 189 cm<sup>2</sup>, while the apparent volume of the cathode was 111 mL with 132 cm<sup>2</sup> geometric  
200 surface area. The novel design was also optimized in the way that the distance between the  
201 anode and cathode also lowered. As the spacing is a major factor in the performance of the  
202 MFC, the lower the spacing between the anode and cathode, the higher will be the efficiency  
203 of the MFC assembly. Being the favourable factor for the performance of the MFC, the spacing  
204 between the anode and cathode has adjusted at 5.5 to 6 mm. The surface-to-volume ratio of  
205 anode and cathode was 1.017 and 1.194 respectively. The copper wire was used as the  
206 connector between the two electrodes (anode and cathode). The copper wire was used due to  
207 its minimum current resistance and maximum level of conductivity as compared to other wires  
208 like titanium and stainless steel.



209

210 For regular electrochemical analysis, copper wire is extensively used for the outside connection  
211 between the two paraboloid cups [27-29]. The voltage and the current of the MFC assembly  
212 were measured by the multi-meter and cyclic voltammetry. In Microbial Fuel Cell (MFC) the  
213 mixed liquor or the mixed microbial consortia was developed from the Municipal Solid  
214 Wastewater (MSW) to develop biocatalyst and biofilm for bio-electrogenic activity in the  
215 wastewater. The MSW contains the mixed microbial consortia which were collected from the  
216 domestic wastewater tank (NFC-IET Multan) with 545 mg/L COD and pH 7.4–7.7. Prior to  
217 the use of MSW into the MFC for the inoculation, 1 L MSW was taken into a beaker and left  
218 it to settle for a certain time at room temperature. When the sewage water was settled down,  
219 the 900 mL of supernatant was removed out and the rest of 100 mL of MSW containing the  
220 sludge was taken into the anode chamber as inoculum. The specific amount of sodium acetate  
221 (3 g/L) was also added in the anode to settle the sludge, which acts as the substrate in the anode  
222 and helped in increasing the growth rate of the bacteria [30, 31].

223

224 The opening of the anode was closed to ensure the anaerobic condition inside the anode, which  
225 was operated for 8 days to enrich the biofilm that will be developed on the inner walls of the  
226 anode in the anodic compartment. The same media which was formulated for the initial step  
227 was also prepared for the next two more cycles with new anodic liquid. The three cycles  
228 ensured a considerable growth of the biofilm inside the anode. On completing the three cycles,  
229 and the formation of the biofilm in the anode, the cathode was introduced into the anode to  
230 receive the electrons from anode without rupturing or disturbing the biofilm.

### 231 **2.3. MFC operation**

232 After the formation of truncated MFC and the development of biofilm in the anodic section,  
233 the operation of MFC started for the treatment of the real wastewater or the effluent of the

234 pharmaceutical industry. The designed MFC was operated for the pharmaceutical wastewater  
235 which contained several wastage constituents of drugs, organic pollutants, syrups and the  
236 residues of the multi-vitamins with COD of 5460 mg/L. The nitrogen gas was supplied for 10  
237 min to the anode to maintain the anaerobic condition [32]. The 65 mL of wastewater (based on  
238 the available volume of the anode that was 70 mL) was taken into the anodic chamber along  
239 with 2 mL of the nutrient solution (the acetate solution) through the sampling opening on the  
240 lid of anode using the syringe. In the cathode chamber, 100 mM of the phosphate buffer  
241 solution having the neutral pH (pH 7) was added as the catholyte to increase the conductivity  
242 (M1000 Benchtop; Thomas Scientific, USA) and maintain the pH for electricity-generating  
243 bacteria [33].

244

245 The cathode was remained open to the air so that the catholyte could have the excess supply of  
246 air to accomplish the reduction reaction which must take place in the cathodic chamber. The  
247 MFC was operated in both modes at the room or ambient temperature ( $22 \pm 2$  °C). The MFC  
248 was operated for 4 days (HRT, the hydraulic retention time), after which the anodic feed of the  
249 first cycle was removed carefully from the anodic chamber with the help of a syringe and the  
250 fresh feed of the same media was added to start the next bath cycle. The operated feed, which  
251 was taken out, was stored in the refrigerator (4 °C) to persevere the actual nature of the treated  
252 feed, and to evaluate the operating performance of the whole system. The MFC reactor was  
253 operated up to 5 cycles in total at the same operating conditions, for evaluating the performance  
254 of the MFC assembly for pharmaceutical wastewater treatment.

#### 255 **2.4. Bio-electrochemical analysis**

256 The performance evaluation of the MFC was considered based on the parameters including  
257 potential difference, open-circuit voltage (OCV), voltage and the current (at different applied  
258 resistances), power (mW), current density (mA/m<sup>2</sup>) and the volumetric power density (W/m<sup>3</sup>).

259 The output parameters such as potential difference or the open-circuit voltage (OCV), voltage,  
260 and the currents were recorded by using the multi-meter [34]. The power density ( $W/m^3$ ) was  
261 calculated with the help of a reaction (**Eq. (4)**). The power density is the amount of power that  
262 is generated per unit area. The power density was measured at anode because all the biological  
263 activities were acquired at the anode.

$$264 \quad P = \frac{I \times V}{A} \quad (4)$$

265  
266 where P represents the power density ( $W/m^3$ ), A is the area of the anode ( $m^2$ ), V is the voltage  
267 (mV) and I represent the flowing current (mA). The current density ( $mA/m^2$ ) was calculated  
268 by following the **Eq. (5)** [35].

$$269 \quad J = \frac{I}{A} \quad (5)$$

270  
271 where J represents the current density ( $mA/m^2$ ), A is the area of the anode ( $m^2$ ), and I represent  
272 the flowing current (mA). The COD was calculated at the end of each cycle in such a way that,  
273 when the feed sample was removed from the MFC, the 50 mL of the sample of PIW was taken  
274 to the COD bottles for measuring the COD of a sample. The COD and TDS were calculated  
275 by using the closed reflux method [36, 37]. Organic loading rate (OLR) is used to calculate the  
276 quantity of influent substrate that enters the digester per unit time and determined using **Eq.**  
277 **(6)**, whereas the substrate degradation rate (SDR) was determined to study the pattern and rate  
278 of COD removal during cycle operation and calculated using the **Eq. (7)**. Both OLR and SDR  
279 have the same units as  $kg\ COD/m^3\ day$  [38].

$$280 \quad OLR = COD_{initial}/HRT \quad (6)$$

$$281 \quad SDR = CRE \times OLR \quad (7)$$

283

284 where HRT is the hydraulic retention time (days),  $COD_{initial}$  is the chemical oxygen demand  
285 (mg/L), and CRE is the COD removal efficiency (%).

286 In the end, the power yield was calculated by relating the maximum power with that of the total  
287 amount of COD which was removed at the end of each cycle.

## 288 **2.5. Cyclic voltammetry**

289 Cyclic voltammetry (CV) was accompanied for evaluating the behaviour of the biocatalyst or  
290 the bio-anode and the electrode interference [39] using the potentiostat model CHI700E (CH  
291 Instruments, USA). The CV experiments were performed using a potentiostat configuration  
292 and five different experimental scenarios. On applying the potential ramp (scan rate and scan  
293 range are specified) the graphs of loop-shaped were obtained when the applied potential was  
294 taken as the values of x-coordinate and the values of open circuit potential were taken as y-  
295 coordinate. In the system, the anode was used as a working electrode and the cathode as a  
296 counter electrode [40], while the wastewater was used as the electrolyte. To measure the  
297 polarization behaviour of the MFC, the current density was taken across the wide range of the  
298 external resistance ranging from 10  $\Omega$  to 30 K $\Omega$ . This polarization behaviour was evaluated  
299 twice, in the first cycle and then in the fifth cycle of operation. The pH and the TDS were  
300 calculated at the end of each cycle [41].

## 301 **3. Results and discussion**

302 The results for pharmaceutical wastewater in paraboloid MFC are much impressive. This  
303 assembly effectively removed up to 80.50% of the COD of pharmaceutical wastewater,  
304 generated up to 2.76 mA current, and the voltage of 0.80 mV. This unique design has given  
305 more area to volume ratio, which is also one of the uniqueness of this design as described in  
306 the following sections.

### 307 **3.1. Pharmaceutical wastewater treatment**

308 Pharmaceutical industry waste contains the phosphate of aminophylline, ammonium chloride,  
309 methanol, certain salts of glycerophosphate, organics and other antiseptics including  
310 chlorhexidine, permanganates, and quaternary ammonium compounds. According to emerging  
311 evidence, the chemical oxygen demand (COD) of the pharmaceutical industry wastewater  
312 (PIW) ranges from 1600–7000 mg/L, this range of (COD) shows the higher amount of the  
313 organics present in the wastewater which has to be treated before discharging out [7]. The  
314 paraboloid shaped microbial fuel cell (MFC) provides the efficient treatment of this effluent  
315 anaerobically.

#### 316 **3.1.1. COD and TDS reduction**

317 The initial COD of collected pharmaceutical wastewater was 5460 mg/L. To reduce the COD  
318 of PIW by MFC, five cycles were performed up to 8 days. During the operation of five cycles,  
319 the minimum 26.92% COD reduction (5460 to 3990 mg/L) was achieved in the first cycle and  
320 maximum COD reduction (5460 to 1060 mg/L) efficiency of about 80.55% of PIW was  
321 achieved in the fifth cycle by MFC. These findings give remarkable pharmaceutical wastewater  
322 treatment efficiency as presented in **Fig. 2**. The findings of **Table.1** reported that during the  
323 first operating cycle, the total 1470 mg/L of COD was removed, and clearly stated that by  
324 increasing the operation cycle the reduction efficiency of COD also increased from 1470 to  
325 4400 mg/L after fifth cycles.

326

327 The findings of the substrate degradation rate (SDR) were improved from 0.36 to 1.09 kg  
328 COD/m<sup>3</sup> day as presented in **Table.1**. The SDR has followed the same trends as COD  
329 reduction, it was improved by increasing the operation cycle. The results are also in agreement  
330 with previously reported findings, Mohan et al., [42] observed the maximum SDR value of

331 0.88 kg COD/m<sup>3</sup> day with 62.9% COD removal for chemical wastewater by dual-chambered  
332 MFC. They also reported the maximum voltage of about 304 mV at an organic loading rate  
333 (OLR) of 1.40 kg COD/m<sup>3</sup> day. Abbasi et al., [18] showed that Perspex glass made MFC  
334 effectively reduced the COD of chemical industry wastewater from 452 to 60 mg/L. They also  
335 revealed that MFC reduced the phosphate concentration in the chemical industrial wastewater  
336 from 52.7 to 35.7 mg/L. Similarly, Amari et al., [33] reported that the 78 and 93% of COD of  
337 synthetic and pharmaceutical plant wastewater was reduced by dual-chamber constructed MFC  
338 (Plexiglas sheet). Furthermore, Ismail and his research group observed that Perspex glass made  
339 microbial fuel cell (MFC) with granular activated carbon (GSC) as biofilm successfully  
340 reduced up to 83% of pharmaceutical wastewater after continuous operation of 45 days [32].

341

342 The organic contents which degraded in the anodic chamber anaerobically produced some  
343 gases including CO<sub>2</sub> as intermediate. The anaerobes (*Shewanella putrefaciens* and *Aeromonas*  
344 *hydrophila*) which were present in the anode utilizes these organic matters through metabolism.  
345 The degradation of the organic matter results in COD reduction that interprets as the function  
346 of treatment of wastewater and is called as wastewater treatment efficiency of MFC. Like COD,  
347 the TDS is also an important factor in the wastewater. During five cycles of operation TDS of  
348 the PIW was also calculated, which was recorded as 800 at an initial stage. The results of  
349 **Table.2** showed the maximum TDS removal efficiency was recorded as 35.64% (800 to 515  
350 mg/L) at the fourth operation cycle whereas the minimum of 33% (800 to 536 mg/L) efficiency  
351 was recorded during the fifth cycle.

352

353 The TDS removal efficiency during the first cycle was recorded as 33.75% (800 to 530 mg/L)  
354 that improved up to the fourth cycle (35.64%). This trend may be due to the complexity of  
355 organic solvents in the actual pharmaceutical wastewater. These results are also in correlation

356 with previously reported findings, Prasad et al., [25] showed the TDS removal from 2600 to  
357 2150 mg/L (17.31%) for pharmaceutical wastewater using dual-chambered MFC. Similarly,  
358 Mahendra and co-workers observed the significant TDS removal from 1000 to 250 mg/L using  
359 MFC [43]. Padmaja et al., [5] reported that the chemical coagulation method using Alum and  
360 FeCl<sub>3</sub> removed the TDS of active pharmaceutical ingredients like 14% (16290 to 14000 mg/L)  
361 and 26.30% (16290 to 12000 mg/L) respectively. Nikhil et al., [44] observed that aerobic  
362 nitrification treatment (ANT) operation on pharmaceutical wastewater treatment effectively  
363 removed the TDS, phosphates and sulfates of about 24.5, 49.6, and 43% respectively. They  
364 also reported that the maximum TDS removal efficiency in the denitrification treatment (DNT)  
365 operation system was recorded as 24.2% during pharmaceutical wastewater treatment. Palani  
366 et al., [45] stated that the membrane bioreactor successfully reduced the Total Dissolved Solids  
367 (TDS) of pharmaceutical wastewater of about 70% at 300 kPa with 35% increased flux.

### 368 **3.2. Bioelectricity generation by MFC**

369 Municipal solid wastewater (MSW) is used for the development of the biofilm, as it contains  
370 the mixed microbial consortium which develops the biofilm on the anode's inner surface  
371 effectively. The COD of the collected MSW was 545 mg/L with a pH 7.4–7.7. The formation  
372 of electroactive bacteria (*Shewanella oneidensis*, *Shewanella putrefaciens* and *Aeromonas*  
373 *hydrophila*) at the anode surface is the basic source of the current generation in MFC, as these  
374 bacteria are in the form of a nano-pili forming sessile layer which helped in the movement of  
375 bacteria via external force. When the metabolism activity of the bacteria starts, it extracts the  
376 electrons to degrade the organic waste present in pharmaceutical wastewater. Cyclic  
377 voltammetry is an electrochemical technique for evaluating out the redox reaction at the surface  
378 of the electrode.

379

380 Bioelectrogenesis and substrate degradation, both can be illustrated using electrochemical  
381 reaction in the MFC. The response of the biofilm was interpreted as a function of current  
382 generation with applied potential, which gradually increases from the first cycle to the fifth  
383 cycle; thus, this improvement in current is the function of bacterial biofilm (*Shewanella*  
384 *oneidensis*, and *Aeromonas hydrophila*) as presented in **Fig. 3**. The discharge rate of the  
385 electrons during the metabolism can be determined by the oxidation and reduction peaks, so  
386 Forward Sweep (FS) and Reverse Sweep (RS) is responsible for it. The cyclic voltammetry of  
387 PIW during all five cycles shows the development of the electroactive biofilm with increasing  
388 the concentration of anolyte and catholyte due to the diffusion. The sharp peaks during the FS  
389 and RS demonstrate the reaction occurring as a result of a redox reaction. Velvizhi and Mohan  
390 [46], stated that the anaerobic operation (ANO) of pharmaceutical wastewater showed the  
391 maximum reduction current of -2.81 mA as compared to the oxidation current as 0.65 mA. But  
392 they also revealed that the bio-electrochemical treatment operation of wastewater showed the  
393 maximum oxidation current of 24.98 mA in contrast to reduced current 23.25 mA.

394  
395 The amount of current generation depends on the surface area of an anode, organic content,  
396 and the types of microorganisms. MFC is operated for 5 cycles up to 8 days. **Fig. 4** illustrated  
397 that the maximum open-circuit voltage (OCV) was recorded as 330 mV after 96 h (4 days)  
398 wastewater treatment by MFC. The initial OCV was measured as 134 mV after 8 h treatment  
399 that effectively increased up to 330 mV after 96 h treatment (4 days), but suddenly it decreased  
400 to 133 mV after 184 h treatment. Sun and co-workers revealed that the actual pharma  
401 wastewater contains much complexity as compared to acetate-containing wastewater because  
402 acetate acts as a simple substrate in the growth of electroactive bacteria [47].

403



404 Velvizhi and Mohan [48] revealed that the maximum 242 mV production of OCV with 54.28  
405 mW/m<sup>2</sup> power density was achieved with DSW (designed synthetic wastewater) as a substrate  
406 during pharmaceutical wastewater treatment by a single-chambered MFC (Perspex glass).  
407 They also reported that the production in open-circuit voltage (OCV) and power density  
408 increased as 290 mV and 118.89 mW/m<sup>2</sup> by increasing the organics load, this may be due to  
409 the availability of higher substrate for the anodic biocatalyst that improved the anolyte  
410 conductivity. The current efficiency (mA), power (mW), and voltage (mV) were evaluated up  
411 to five operating cycles, and each cycle comprises for 4 days. Each parameter was recorded  
412 after every 8 h.

413

414 The maximum amount of current generation in the first, second, third, fourth, fifth cycle was  
415 achieved as 1.94, 2.13, 2.35, 2.56, 2.76 mA, respectively as presented in **Fig. 5** and **Fig. 6**,  
416 which illustrates the production of voltage during PIW treatment in MFC. The maximum  
417 voltage in the first cycle was recorded as 194 mV, followed by 213, 235, 256, and 276 for  
418 second, third, fourth, and fifth cycles respectively. The results clearly showed that the overall  
419 maximum voltage as 276 mV was produced in the 5<sup>th</sup> cycle after 440 h treatment. The current  
420 and voltage that are produced during the five cycles are the function of biofilm growth, which  
421 depends on the thickness of the biofilm. The more thickness of biofilm, the more will be the  
422 current and voltage produced. As the biofilm thickness increases on the anodic surface, the  
423 current and voltage produced also increase, which is called the electroactive enrichment.

424

425 Similarly, **Fig. 5** illustrate the production of power, the maximum power during the 1<sup>st</sup>, 2<sup>nd</sup>, 3<sup>rd</sup>,  
426 4<sup>th</sup> and 5<sup>th</sup> operated cycle was achieved as 0.37, 0.45, 0.55, 0.65 and 0.76 mW respectively.  
427 These results are also in agreement with previous reported MFC and conventional methods for  
428 pharmaceutical wastewater treatment. Huggins et al., [49] reported that graphite made

429 microbial fuel cell (aeration reactor) generated the maximum power of 0.36 Wh equivalent to  
430 24 Wh per cubic meter pharmaceutical wastewater treatment followed by 135 mV voltage and  
431 193 mA/m<sup>2</sup> power density production. Naik et al., [35] demonstrated that dual chambered MFC  
432 effectively produced the voltage of 0.8 V for 144 h treatment of wastewater. They reported that  
433 the maximum 68 mA current was also produced till 168 h.

### 434 **3.2.1. Power and current densities**

435 In MFC, some amount of total produced power can be lost more than one source, that can  
436 minimize the total ideal voltage production, and cause activation and concentration losses,  
437 which are termed as internal resistance [50]. Internal resistance was calculated by using the  
438 polarization curve. The polarization curve was drawn by varying the external resistance from  
439 OCV (open circuit voltage) to the SCV (short circuit voltage) when a steady state of voltage  
440 was reached across 100  $\Omega$  resistance. The internal resistance of the MFC was equal to the  
441 external resistance when maximum power density reached (1.47 W/m<sup>3</sup>) or by the slope of the  
442 V-I graph ( $R=\Delta V/\Delta I$ ).

443  
444 The polarization curve was recorded at the end of two cycles (1<sup>st</sup> and 5<sup>th</sup> cycle) with the external  
445 resistance of 10 to 30 k $\Omega$ . The polarization curve which was recorded during the first cycle,  
446 gives the maximum power density of 1.47 (W/m<sup>3</sup>), with a maximum current density of 37.18  
447 (mA/ m<sup>2</sup>) across 197  $\Omega$  resistor, as the internal resistance of the MFC in the first cycle was  
448 recorded 197  $\Omega$ , as shown in **Fig. 7**. Initially, the power density increased from 0 to 1.47 W/m<sup>3</sup>  
449 but after it starts to decrease from 1.47 to 1.15 W/m<sup>3</sup> but current density increased from 0 to  
450 146.5 mA/m<sup>2</sup> with reducing the resistance from 3000 to 10  $\Omega$ . **Fig. 8** demonstrate the  
451 production of current density and power density. The polarization curve which was recorded  
452 during the 5<sup>th</sup> cycle gives the maximum power density of 2.01 (W/m<sup>3</sup>), a maximum current

453 density of 168.05 (mA/m<sup>2</sup>) across 99 Ω resistor, as the internal resistance of the MFC in 5<sup>th</sup>  
454 cycle was recorded 99 Ω, as presented in **Fig. 8**.

455

456 The overall findings indicate that the maximum power and current densities of about 2.01  
457 W/m<sup>3</sup> and 168.05 mA/m<sup>2</sup> were achieved after the 5<sup>th</sup> operation cycle of MFC in PIW treatment,  
458 which may be due to the availability of acetate as a substrate that gives more biodegradability.  
459 Velvizhi and his co-workers showed that bio-electrochemical treatment (BET) operation of  
460 pharmaceutical wastewater generated a maximum of 81.67 mW/m<sup>2</sup> and 371 mA/m<sup>2</sup> power  
461 density (PD) and current density (CD) respectively at lower organic load. They stated that total  
462 PD (157.60 mW/m<sup>2</sup>) and CD (508.60 mA/m<sup>2</sup>) production increased by increasing the organic  
463 load. They also reported that the anaerobic operation of pharmaceutical wastewater treatment  
464 only produced current with electron membrane assembly during bio-electrochemical analysis  
465 [46].

466

467 Chang et al. [51] reported that the maximum power density (PD) and coulombic efficiency  
468 (CE) of about 162.74 mW/m<sup>2</sup> and 7.09% were recorded after 8 h of HRT (hydraulic retention  
469 time) by MFC (plain-graphite plate) during pharmaceutical wastewater treatment containing  
470 PPs. They also revealed that the total PD and CE production decreased to 29.12 mW/m<sup>2</sup> and  
471 2.23% respectively after 5 h HRT in sewage water. Nayak and his research group reported that  
472 the MFC wastewater treatment system generated the maximum power density of about 560.81  
473 mW/m<sup>2</sup> and voltage of about 610 mV after 21 day treatment [52]. The power density of  
474 paraboloid shaped-designed MFC is the function of the cathode surface area (0.023 m<sup>2</sup>),  
475 electrode spacing, and the growth of biofilm. The spacing between the electrodes was 6 mm.  
476 The polarization curves during all the five cycles show that the volumetric power density has  
477 increased from 1.46 to 2.01 W/m<sup>3</sup> and reduced the internal resistance from 197 to 99 Ω due to

478 the enrichment of the biofilm. Under the current scenario of environmental pollution [53, 54],  
479 there is serious need to develop and apply eco-green technologies [55] to tackle the pollution  
480 [56] therefore, microbial fuel cells could be an excellent options for the treatment of diverse  
481 type of wastewater micropollutants as well as to generate bioelectricity.

## 482 **4. Conclusions**

483 With the growing world population, the environmental regulatory agencies have put the  
484 researchers on the way to evolve or to present some unique methods and technologies for the  
485 better development of human beings. In the present study, the novel graphite-based paraboloid  
486 shaped Microbial Fuel Cell (MFC) was built to treat the pharmaceutical wastewater and  
487 generate electricity. The MFC analysis was performed up to five operating cycles for 8 days  
488 for the treatment of pharmaceutical industrial waste. The newly designed, truncated paraboloid  
489 MFC gives a higher surface area of about  $0.023 \text{ m}^2$  per unit volume with the minimum electrode  
490 spacing which was found to be the feasible and favourable technology for energy production  
491 and wastewater treatment. The results demonstrated that the MFC analysis significantly  
492 reduced the COD and TDS of pharmaceutical wastewater of about 80.55 and 35.23%  
493 respectively. The cyclic voltammetry findings reported that the truncated paraboloid MFC  
494 successfully generated a power density of  $2.01 \text{ W/m}^3$  along with reducing the internal  
495 resistance from 197 to  $99 \Omega$  after the five operating cycles. The MFC technique effectively  
496 generated the maximum open-circuit voltage (OCV) of 330 mV after 96 h treatment, followed  
497 by current, power, and voltage of about 2.76 mA, 0.76 mW, and 276 mV after 440 h treatment  
498 respectively. Moreover, biofilm development during the five cycles with reducing the internal  
499 resistance along with COD removal and substrate degradation rate showed the upscaling  
500 viability of the microbial fuel cell (MFC) also at the commercial level. However, it is  
501 recommended that the current density and the power density should be increased, by using the  
502 natural or the synthesized mediators, these mediators might increase the electron extract ratio

503 from the cell of microbes. In pharmaceutical industrial wastewater along with various organic  
504 chemicals, the effluent also contains antiseptics. So, it is also suggested that researchers should  
505 have to work on these antiseptics, for enhancing the efficiency of the microbial fuel cell (MFC).

## 506 **Acknowledgement**

507 The authors are thankful to the Higher Education Commission of Pakistan for the financial  
508 support to carry on this research.

509

510

## 511 References

- 512 1. Chen, X., et al., Pharmaceutical Industry in China: Policy, Market and IP, in *Innovation,*  
513 *Economic Development, and Intellectual Property in India and China.* 2019, Springer.  
514 p. 215-250.
- 515 2. Kusui, T., Y. Itatsu, and J. Jin, Whole Effluent Toxicity Assessment of Industrial  
516 Effluents, in *Toxicity and Biodegradation Testing.* 2018, Springer. p. 331-347.
- 517 3. Singal, N. and S. Kaur, Review on physico-chemical analysis of various pharmaceutical  
518 industrial effluents & its impact on the environment. *International Journal of Science*  
519 *Applied Research*, 2018. 5: p. 07-11.
- 520 4. Sher, F., et al., Implications of advanced wastewater treatment: Electrocoagulation and  
521 electroflocculation of effluent discharged from a wastewater treatment plant. *Journal of*  
522 *Water Process Engineering*, 2020. 33: p. 101101.
- 523 5. Padmaja, K., J. Cherukuri, and M.A. Reddy, A comparative study of the efficiency of  
524 chemical coagulation and electrocoagulation methods in the treatment of  
525 pharmaceutical effluent. *Journal of Water Process Engineering*, 2020. 34: p. 101153.
- 526 6. Li, H., et al., Accumulation of sulfonamide resistance genes and bacterial community  
527 function prediction in microbial fuel cell-constructed wetland treating pharmaceutical  
528 wastewater. *Chemosphere*, 2020. 248: p. 126014.
- 529 7. Bagchi, S. and M. Behera, Pharmaceutical wastewater treatment in microbial fuel cell,  
530 in *Integrated Microbial Fuel Cells for Wastewater Treatment.* 2020, Elsevier. p. 135-  
531 155.
- 532 8. Sher, F., A. Malik, and H. Liu, Industrial polymer effluent treatment by chemical  
533 coagulation and flocculation. *Journal of Environmental Chemical Engineering*, 2013.  
534 1(4): p. 684-689.
- 535 9. Changotra, R., et al., Techno-economical evaluation of coupling ionizing radiation and  
536 biological treatment process for the remediation of real pharmaceutical wastewater.  
537 *Journal of Cleaner Production*, 2020. 242: p. 118544.
- 538 10. Maimon, A. and A. Gross, Greywater: Limitations and perspective. *Current Opinion in*  
539 *Environmental Science Health*, 2018. 2: p. 1-6.
- 540 11. Wang, H., et al., Removal and fate of trace organic compounds in microbial fuel cells.  
541 *Chemosphere*, 2015. 125: p. 94-101.
- 542 12. Martinez-Alcala, I., J.M. Guillén-Navarro, and C. Fernandez-Lopez, Pharmaceutical  
543 biological degradation, sorption and mass balance determination in a conventional  
544 activated-sludge wastewater treatment plant from Murcia, Spain. *Chemical*  
545 *Engineering Journal*, 2017. 316: p. 332-340.
- 546 13. Haldar, D., et al., Microbial Fuel Cell for the Treatment of Wastewater. *Microbial Fuel*  
547 *Cells: Materials Applications.* Vol. 46. 2019. 289-306.
- 548 14. Dannys, E., et al., Wastewater treatment with microbial fuel cells: a design and  
549 feasibility study for scale-up in microbreweries. *J Bioprocess Biotech*, 2016. 6(267): p.  
550 2.
- 551 15. Ye, Y., et al., Effect of organic loading rate on the recovery of nutrients and energy in  
552 a dual-chamber microbial fuel cell. *Bioresource technology*, 2019. 281: p. 367-373.
- 553 16. Nayak, J.K. and U.K. Ghosh, Microalgae Cultivation for Pretreatment of  
554 Pharmaceutical Wastewater Associated with Microbial Fuel Cell and Biomass Feed  
555 Stock Production, in *Frontiers in Water-Energy-Nexus—Nature-Based Solutions,*  
556 *Advanced Technologies and Best Practices for Environmental Sustainability.* 2020,  
557 Springer. p. 383-387.
- 558 17. Wei, J., P. Liang, and X. Huang, Recent progress in electrodes for microbial fuel cells.  
559 *Bioresource technology*, 2011. 102(20): p. 9335-9344.

- 560 18. Abbasi, U., et al., Anaerobic microbial fuel cell treating combined industrial  
561 wastewater: Correlation of electricity generation with pollutants. *Bioresource*  
562 *technology*, 2016. 200: p. 1-7.
- 563 19. Zhuang, L., et al., Scalable microbial fuel cell (MFC) stack for continuous real  
564 wastewater treatment. *Bioresource technology*, 2012. 106: p. 82-88.
- 565 20. Mohanakrishna, G., et al., Cylindrical graphite based microbial fuel cell for the  
566 treatment of industrial wastewaters and bioenergy generation. *Bioresource technology*,  
567 2018. 247: p. 753-758.
- 568 21. Flimban, S.G., et al., The effect of Nafion membrane fouling on the power generation  
569 of a microbial fuel cell. *International Journal of Hydrogen Energy*, 2020. 45(25): p.  
570 13643-13651.
- 571 22. Cheng, S. and B.E. Logan, Increasing power generation for scaling up single-chamber  
572 air cathode microbial fuel cells. *Bioresource technology*, 2011. 102(6): p. 4468-4473.
- 573 23. Kumar, R., L. Singh, and A. Zularisam, *Microbial fuel cells: types and applications, in*  
574 *Waste Biomass Management—A Holistic Approach*. 2017, Springer. p. 367-384.
- 575 24. An, J., et al., Shift of voltage reversal in stacked microbial fuel cells. *Journal of Power*  
576 *Sources*, 2015. 278: p. 534-539.
- 577 25. Prasad, M., et al., Treatment of pharmaceutical industrial effluent by microbial fuel cell  
578 (MFC). *International Journal for Innovative Research in Science Technology*, 2015.  
579 2(1): p. 241-247.
- 580 26. Amari, S. and M. Boshrouyeh Ghandashtani, Non-steroidal anti-inflammatory  
581 pharmaceutical wastewater treatment using a two-chambered microbial fuel cell. *Water*  
582 *Environment Journal*, 2020. 34(3): p. 413-419.
- 583 27. Manjerkar, Y., S. Kakkar, and A. Durve-Gupta, Bio-Electricity Generation Using  
584 Kitchen Waste And Molasses Powered MFC, in *National Conference on 'Advanced*  
585 *Analytical Tools for Materials Characterization'*. 2018. p. 181-187.
- 586 28. Prasad, J. and R.K. Tripathi. Maximum electricity generation from low cost sediment  
587 microbial fuel cell using copper and zinc electrodes. in *2017 International Conference*  
588 *on Information, Communication, Instrumentation and Control (ICICIC)*. 2017. IEEE.
- 589 29. Patel, R., et al., Microbial Fuel Cell Laboratory Setup, in *Adaptive and Intelligent*  
590 *Control of Microbial Fuel Cells*. 2020, Springer. p. 99-108.
- 591 30. Bi, L., et al., One-step pyrolysis route to three dimensional nitrogen-doped porous  
592 carbon as anode materials for microbial fuel cells. *Applied Surface Science*, 2018. 427:  
593 p. 10-16.
- 594 31. Kumar, R., L. Singh, and A. Zularisam, Exoelectrogens: recent advances in molecular  
595 drivers involved in extracellular electron transfer and strategies used to improve it for  
596 microbial fuel cell applications. *Renewable Sustainable Energy Reviews*, 2016. 56: p.  
597 1322-1336.
- 598 32. Ismail, Z.Z. and A.A. Habeeb, Experimental and modeling study of simultaneous  
599 power generation and pharmaceutical wastewater treatment in microbial fuel cell based  
600 on mobilized biofilm bearers. *Renewable energy*, 2017. 101: p. 1256-1265.
- 601 33. Amari, S. and M. Boshrouyeh Ghandashtani, Non-steroidal anti-inflammatory  
602 pharmaceutical wastewater treatment using a two-chambered microbial fuel cell. *Water*  
603 *Environment Journal*, 2019.
- 604 34. Khalid, S., et al., Dye degradation and electricity generation using microbial fuel cell  
605 with graphene oxide modified anode. *Materials Letters*, 2018. 220: p. 272-276.
- 606 35. Naik, S. and S.E. Jujavarappu, Simultaneous bioelectricity generation from cost-  
607 effective MFC and water treatment using various wastewater samples. *Environmental*  
608 *Science Pollution Research*, 2019: p. 1-11.

- 609 36. Joanna, B.-Z., et al., Cost-Effective Removal of COD in the Pre-treatment of  
610 Wastewater from Paper Industry, in *Frontiers in Water-Energy-Nexus—Nature-Based*  
611 *Solutions, Advanced Technologies and Best Practices for Environmental*  
612 *Sustainability*. 2020, Springer. p. 473-475.
- 613 37. Dash, S.S., R. Subramani, and D.S. Kompala, Method for rapid treatment of waste  
614 water and a composition thereof. 2017, Google Patents.
- 615 38. Mohan, S.V., V.L. Babu, and P. Sarma, Anaerobic biohydrogen production from dairy  
616 wastewater treatment in sequencing batch reactor (AnSBR): effect of organic loading  
617 rate. *Enzyme Microbial Technology*, 2007. 41(4): p. 506-515.
- 618 39. Al-Shara, N.K., et al., Electrochemical study of different membrane materials for the  
619 fabrication of stable, reproducible and reusable reference electrode. *Journal of Energy*  
620 *Chemistry*, 2020. 49: p. 33-41.
- 621 40. Al-Shara, N.K., et al., Electrochemical investigation of novel reference electrode Ni/Ni  
622 (OH)<sub>2</sub> in comparison with silver and platinum inert quasi-reference electrodes for  
623 electrolysis in eutectic molten hydroxide. *International Journal of Hydrogen Energy*,  
624 2019. 44(50): p. 27224-27236.
- 625 41. López Zavala, M.Á., et al., Use of Cyclic Voltammetry to Describe the Electrochemical  
626 Behavior of a Dual-Chamber Microbial Fuel Cell. *Energies*, 2019. 12(18): p. 3532.
- 627 42. Mohan, S.V., et al., Bioelectricity generation from chemical wastewater treatment in  
628 mediatorless (anode) microbial fuel cell (MFC) using selectively enriched hydrogen  
629 producing mixed culture under acidophilic microenvironment. *Biochemical*  
630 *Engineering Journal*, 2008. 39(1): p. 121-130.
- 631 43. Mahendra, B. and S. Mahavarkar, Treatment of wastewater and electricity generation  
632 using microbial fuel cell technology. *International Journal of Research in Engineering*  
633 *Technology*, 2013: p. 277-282.
- 634 44. Nikhil, G., et al., Energy-positive nitrogen removal of pharmaceutical wastewater by  
635 coupling heterotrophic nitrification and electrotrophic denitrification. *Chemical*  
636 *Engineering Journal*, 2017. 326: p. 715-720.
- 637 45. Palani, K.N., et al., Development of integrated membrane bioreactor and numerical  
638 modeling to mitigate fouling and reduced energy consumption in pharmaceutical  
639 wastewater treatment. *Journal of Industrial Engineering Chemistry*, 2019. 76: p. 150-  
640 159.
- 641 46. Velvizhi, G. and S.V. Mohan, Biocatalyst behavior under self-induced electrogenic  
642 microenvironment in comparison with anaerobic treatment: evaluation with  
643 pharmaceutical wastewater for multi-pollutant removal. *Bioresource technology*, 2011.  
644 102(23): p. 10784-10793.
- 645 47. Sun, M., et al., Manipulating the hydrogen production from acetate in a microbial  
646 electrolysis cell–microbial fuel cell-coupled system. *Journal of Power Sources*, 2009.  
647 191(2): p. 338-343.
- 648 48. Velvizhi, G. and S.V. Mohan, Electrogenic activity and electron losses under increasing  
649 organic load of recalcitrant pharmaceutical wastewater. *International Journal of*  
650 *Hydrogen Energy*, 2012. 37(7): p. 5969-5978.
- 651 49. Huggins, T., et al., Energy and performance comparison of microbial fuel cell and  
652 conventional aeration treating of wastewater. *Microbial and Biochemical Technology*,  
653 2013. 6(2): p. 1-5.
- 654 50. Al-Shara, N.K., et al., Design and optimization of electrochemical cell potential for  
655 hydrogen gas production. *Journal of Energy Chemistry*, 2021. 52: p. 421-427.
- 656 51. Chang, T.-J., et al., Effect of hydraulic retention time on electricity generation using a  
657 solid plain-graphite plate microbial fuel cell anoxic/oxic process for treating



- 658 pharmaceutical sewage. *Journal of Environmental Science Health, Part A*, 2018.  
659 53(13): p. 1185-1197.
- 660 52. Nayak, J.K. and U.K. Ghosh, Microalgal remediation of anaerobic pretreated  
661 pharmaceutical wastewater for sustainable biodiesel production and electricity  
662 generation. *Journal of Water Process Engineering*, 2020. 35: p. 101192.
- 663 53. Sehar, S., et al., Thermodynamic and kinetic study of synthesised graphene oxide-CuO  
664 nanocomposites: A way forward to fuel additive and photocatalytic potentials. *Journal*  
665 *of Molecular Liquids*, 2020: p. 113494.
- 666 54. Kausar, A., et al., Biocomposite of sodium-alginate with acidified clay for wastewater  
667 treatment: Kinetic, equilibrium and thermodynamic studies. *International Journal of*  
668 *Biological Macromolecules*, 2020.
- 669 55. Rashid, T., et al., Formulation of Zeolite-supported Nano-metallic Catalyst and its  
670 Application in Textile Effluent Treatment. *Journal of Environmental Chemical*  
671 *Engineering*, 2020: p. 104023.
- 672 56. Rasheed, T., et al., Surfactants-based remediation as an effective approach for removal  
673 of environmental pollutants—A review. 2020: p. 113960.  
674  
675

676  
677  
678  
679  
680  
681

## List of Tables

<b>Table.1.</b> The COD removal, OLR, and SRD efficiencies of pharmaceutical wastewater treatment by MFC after five operating cycles. ....	27
<b>Table.2.</b> The TDS percentage removal efficiency of pharmaceutical industrial wastewater (PIW) by MFC up to five operating cycles.....	28

682 **Table.1.** The COD removal, OLR, and SRD efficiencies of pharmaceutical wastewater  
683 treatment by MFC after five operating cycles.

Cycle	COD initial	COD final	CRE (%)	HRT (day)	OLR (kg COD/m <sup>3</sup> day)	SDR (kg COD/m <sup>3</sup> day)	COD <sub>R</sub>
1	5460	3990	26.92	4	1.37	0.37	1470
2	5460	2980	45.42	4	1.36	0.61	2480
3	5460	2100	61.54	4	1.35	0.83	3360
4	5460	1500	72.53	4	1.35	0.97	3960
5	5460	1060	80.58	4	1.36	1.09	4400

684 COD: chemical oxygen demand; OLR: organic loading rate; SDR: substrate degradation rate;

685 CRE: COD removal efficiency.

686

687 **Table.2.** The TDS percentage removal efficiency of pharmaceutical industrial wastewater  
688 (PIW) by MFC up to five operating cycles.

Cycle	TDS <sub>initial</sub>	TDS <sub>final</sub>	TDS <sub>R</sub>	TDS removal (%)
1	800	530	270	33.75
2	800	521	279	34.87
3	800	528	272	34.00
4	800	515	285	35.62
5	800	536	264	33.00

689 TDS: Total dissolved solids.

690

691  
692  
693  
694  
695  
696  
697  
698  
699  
700  
701  
702  
703  
704  
705  
706  
707  
708  
709

## List of Figures

**Fig. 1.** The novel configuration of graphite-based paraboloid microbial fuel cells for pharmaceutical wastewater treatment and bioelectrogenesis. ....30

**Fig. 2.** The COD percentage removal efficiency of pharmaceutical wastewater by MFC up to five operating cycles. ....31

**Fig. 3.** The cycle voltammetry analysis of PIW during the 1<sup>st</sup> and 5<sup>th</sup> operating cycles by MFC at bacterial biofilm. ....32

**Fig. 4.** The open-circuit voltage (OCV) generation during the municipal solid wastewater treatment by a microbial fuel cell. ....33

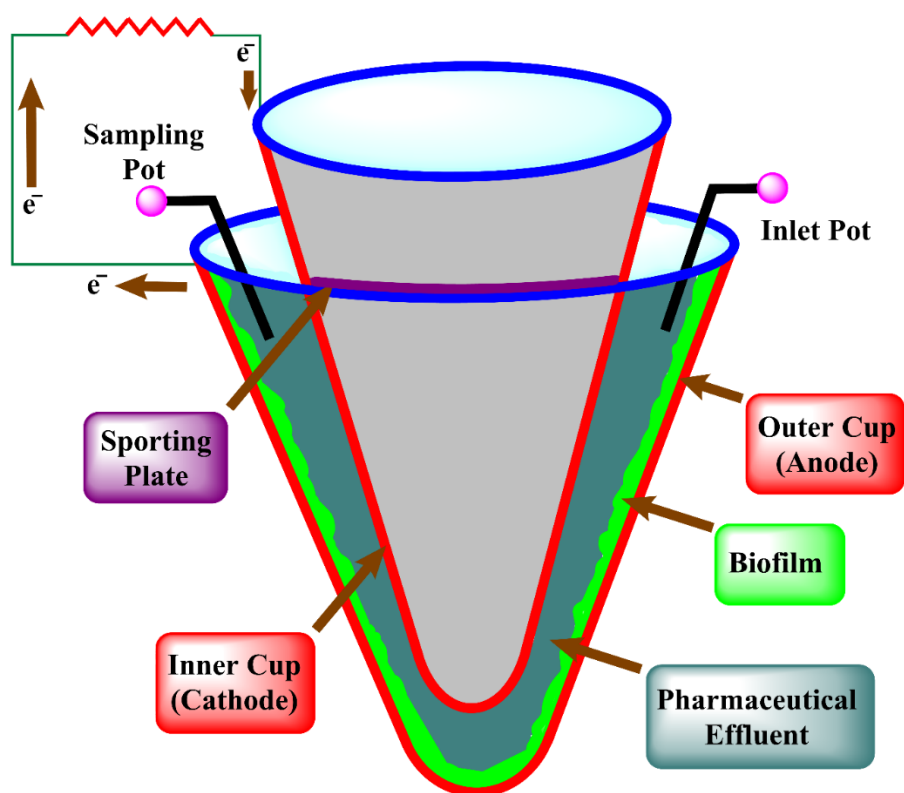
**Fig. 5.** The power and current generation with time during the municipal solid wastewater treatment by microbial fuel cell after five operation cycles. ....34

**Fig. 6.** The total voltage production after five operation cycles during the treatment of PIW by MFC up to 492 h. ....35

**Fig. 7.** The production of power density, current density, and voltage by the 1st operation cycle during the bioelectrogenesis of PIW by MFC. ....36

**Fig. 8.** The production of power density, current density, and voltage by the 5th operation cycle during the bioelectrogenesis of PIW by MFC. ....37

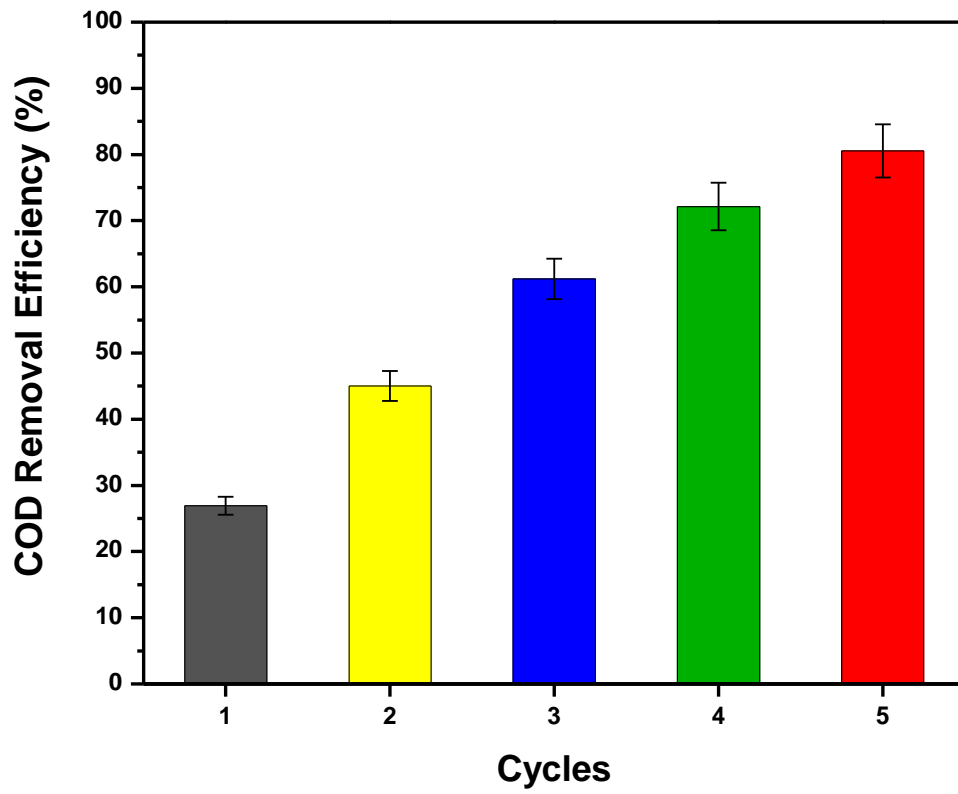
710



711

712 **Fig. 1.** The novel configuration of graphite-based paraboloid microbial fuel cells for  
713 pharmaceutical wastewater treatment and bioelectrogenesis.

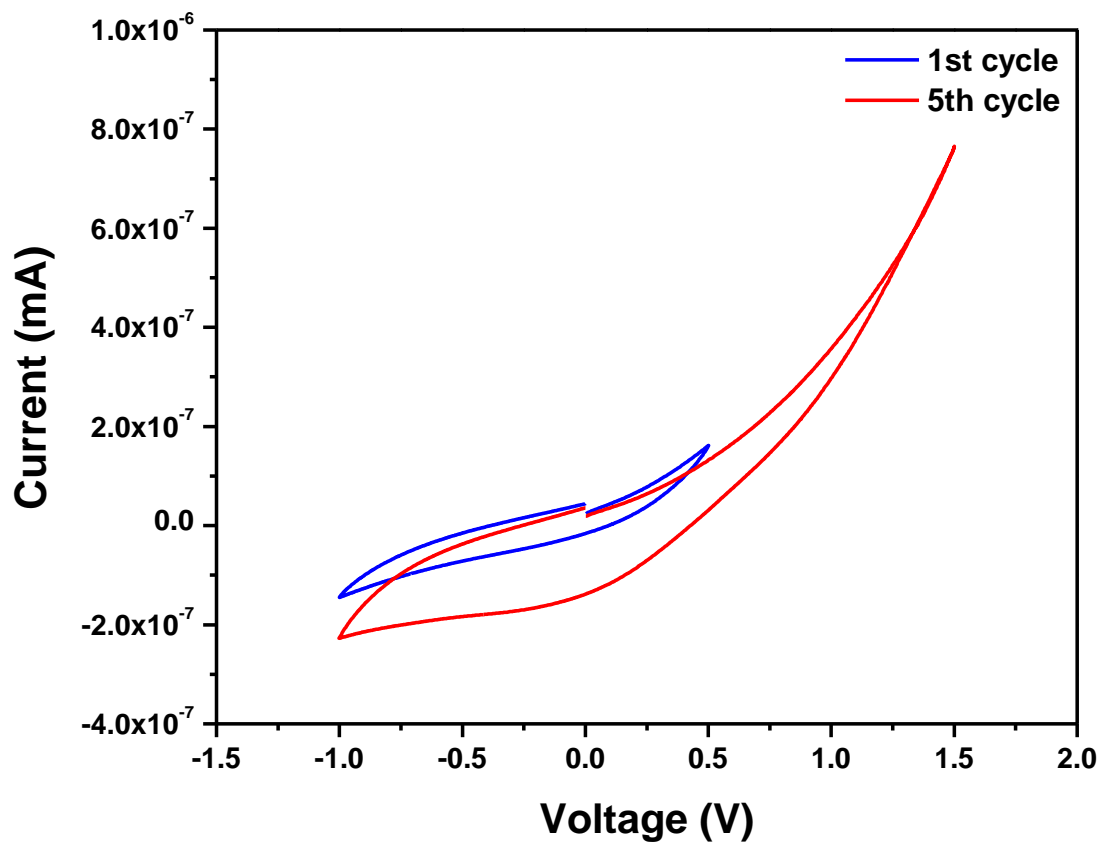
714



715

716 **Fig. 2.** The COD percentage removal efficiency of pharmaceutical wastewater by MFC up to  
717 five operating cycles.

718

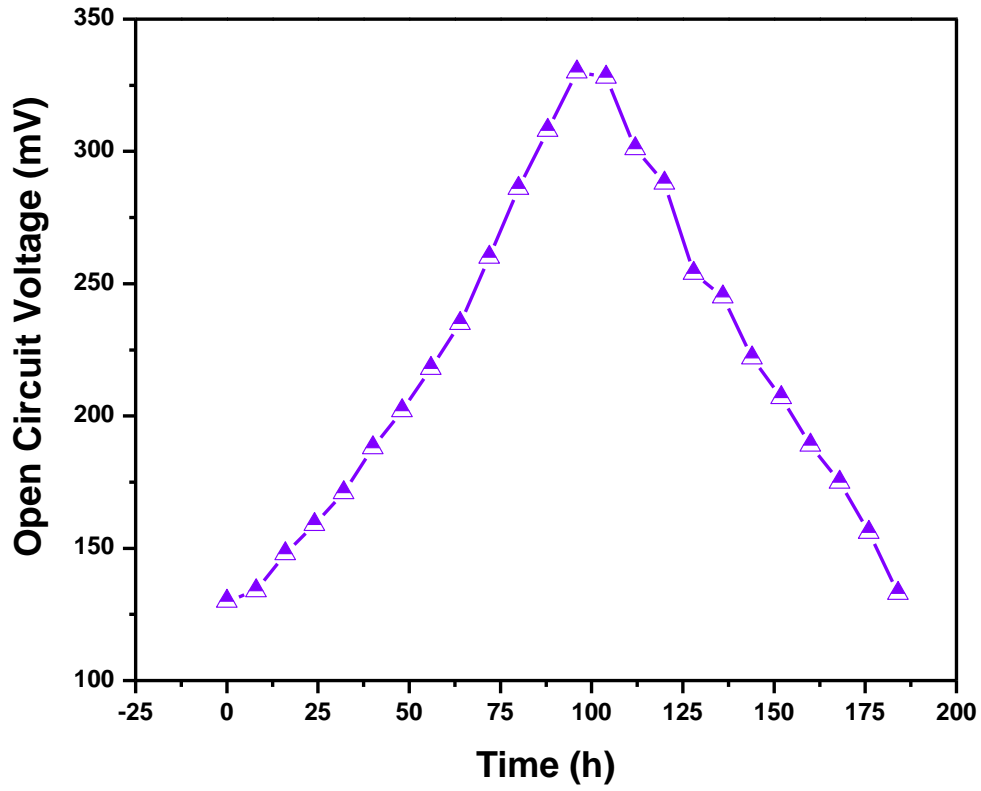


719

720 **Fig. 3.** The cycle voltammetry analysis of PIW during the 1<sup>st</sup> and 5<sup>th</sup> operating cycles by MFC  
721 at bacterial biofilm.

722

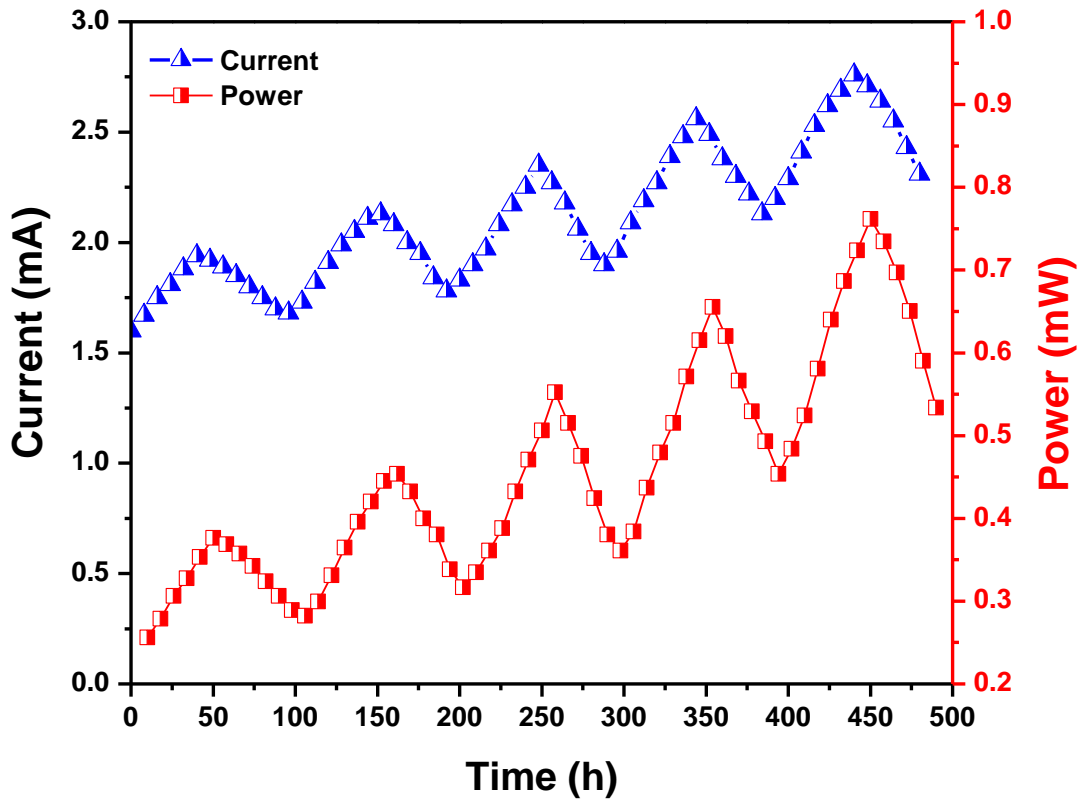




723

724 **Fig. 4.** The open-circuit voltage (OCV) generation during the municipal solid wastewater  
725 treatment by a microbial fuel cell.

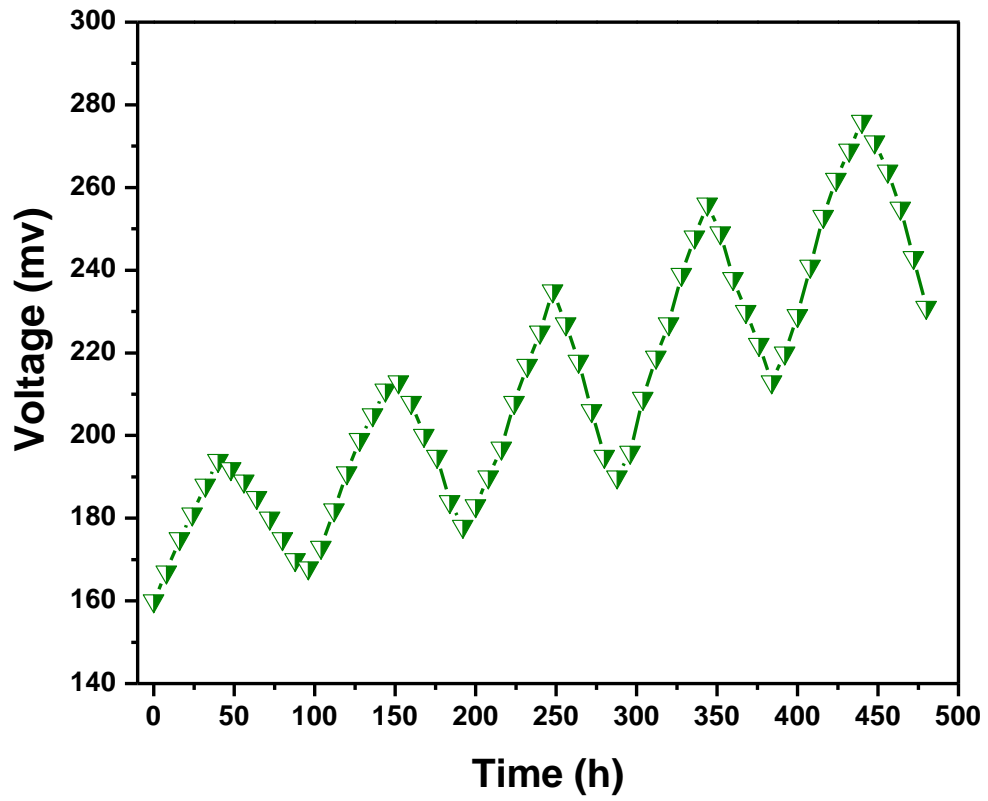
726



727

728 **Fig. 5.** The power and current generation with time during the municipal solid wastewater  
 729 treatment by microbial fuel cell after five operation cycles.

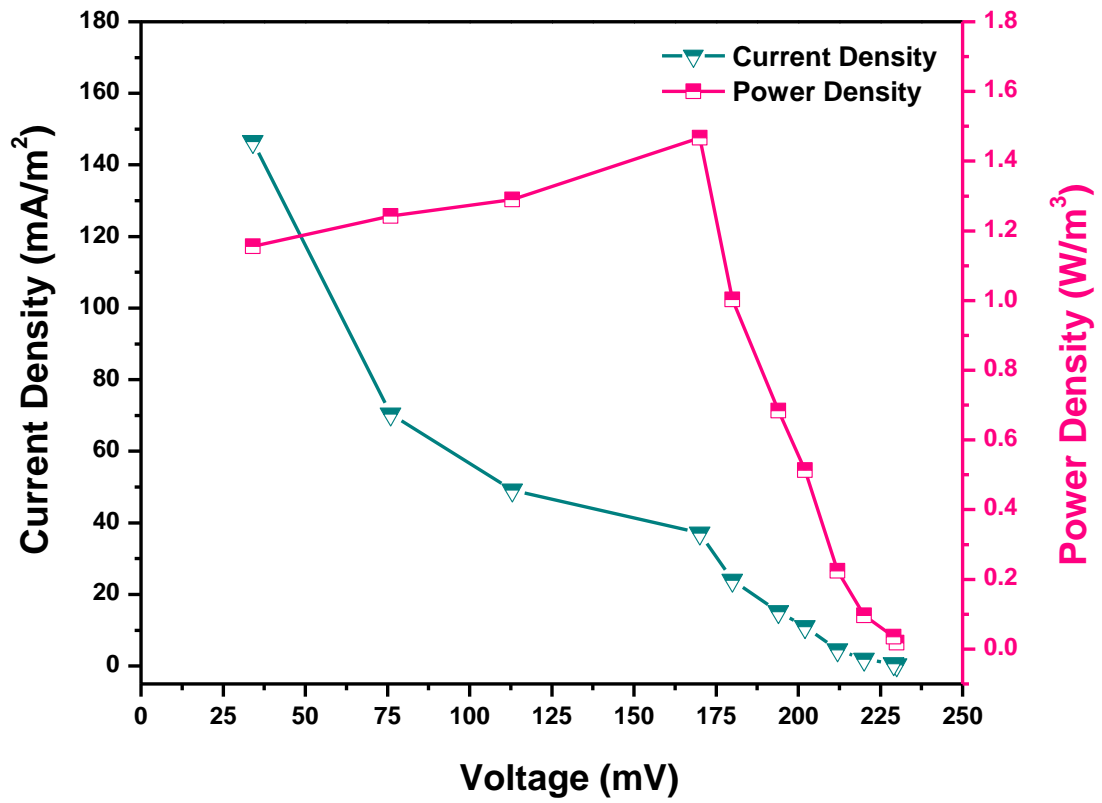
730



731

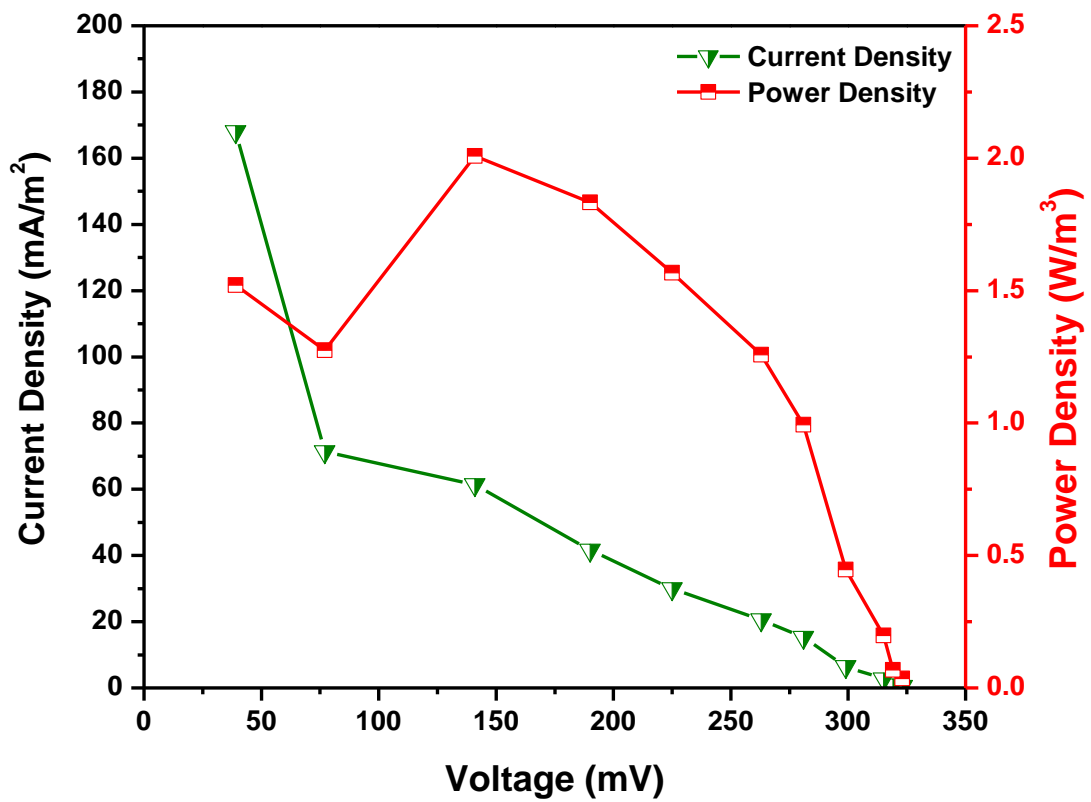
732 **Fig. 6.** The total voltage production after five operation cycles during the treatment of PIW by  
 733 MFC up to 492 h.

734



735

736 **Fig. 7.** The production of power density, current density, and voltage by the 1st operation cycle  
 737 during the bioelectrogenesis of PIW by MFC.  
 738



739

740 **Fig. 8.** The production of power density, current density, and voltage by the 5th operation cycle  
 741 during the bioelectrogenesis of PIW by MFC.  
 742